Liquid Crystals
Publication details, including instructions for authors and subscription information:
http://www.informaworld.com/smpp/title~content=t713926090

Mesomorphic bipyridine building blocks bearing an sp^3 carbon and a hydroxy function

Laurent Douce; Raymond Ziessel; Hsuan-Hong Lai; Hong-Cheu Lin

Online publication date: 06 August 2010

To cite this Article Douce, Laurent , Ziessel, Raymond , Lai, Hsuan-Hong and Lin, Hong-Cheu(1999) 'Mesomorphic bipyridine building blocks bearing an sp^3 carbon and a hydroxy function', Liquid Crystals, 26: 12, 1797 — 1803
To link to this Article: DOI: 10.1080/026782999203427
URL: http://dx.doi.org/10.1080/026782999203427

LIQUID CRYSTALS, 1999, VOL. 26, NO. 12, 1797–1803

Mesomorphic bipyridine building blocks bearing an sp^3 carbon and a hydroxy function

LAURENT DOUCE*, RAYMOND ZIESSEL*

Laboratoire de Chimie, d'Electronique et de Photonique Moléculaires, E.C.P.M./U.P.R.E.S.-A 7008 C.N.R.S. 25, rue Becquerel, 67087 Strasbourg Cedex 2, France

HSUAN-HONG LAI and HONG-CHEU LIN*

Institute of Chemistry, Academia Sinica, Taipei, Taiwan ROC

(*Received 25 May 1999; accepted 31 July 1999*)

The synthesis of novel symmetrical liquid crystalline compounds based on 5-methyl-5′-[2-(4-alkyloxyphenyl)-2-hydroxyethyl]-2,2′-bipyridines is reported, together with some physical properties. Although the chelating head-groups are connected via a chiral sp^3 carbon atom, all the materials are mesomorphic. Intermolecular hydrogen bonding between pyridino and hydroxy fragments in the mesophases is made apparent by FTIR spectroscopy.

1. Introduction

There is much current interest in the preparation of chiral liquid crystalline materials, owing to their physical properties (e.g. thermochromism, ferroelectricity, non-linear optics, pyro- and piezo-electricity) and to their potential applications in display devices, optical data storage systems and thermal sensors [1]. During the last decade, considerable effort has been devoted to the study of metallomesogens since such materials combine attractive features of the metallic centre with those of the mesophase [2]. Surprisingly, there are very few known mesomorphic organometallic compounds built around a chiral centre [3]. In an attempt to overcome this deficiency, we have extended earlier work on oligo-pyridino-based chelates to include the development of potential chiral liquid crystalline materials that form upon coordination to suitable transition metal cations. It should be noted that oligopyridines (e.g. bipyridine, phenanthroline, terpyridine) are very attractive scaffolds for assembling such intricate materials, because they form stable complexes of well-defined geometry with an inordinately rich variety of transition metals in various oxidation states.

Thermotropic liquid crystalline polymers based on homopolyesters of 5,5′-disubstituted-2,2′-bipyridine or alkoxy derivatives of 6,6′-diamino-2,2′-bipyridine, and their corresponding metal [M = Cu(II), Ni(II), Co(II), and Pd(II)] complexes, have been described previously [4]. Furthermore, symmetrical and disymmetrical bipyridines functionalized at the 4,4′- and 5,5′-positions with ester, ethenylene or ethynylene groups, and their mesomorphic complexes, are known to display interesting polymorphic properties [5–8]. In particular, an unusual type of molecular ordering has been reported for a family of liquid crystalline cyclopalladated/bipyridine complexes [7], while the ability of certain cations to induce macroscopic ordering of non-mesomorphic bipyridine modules has been described [8]. It seems reasonable to suppose that such bipyridino modules could be converted into chiral building blocks simply by adding appropriate functional groups into the connecting linkage. In this respect we note that hydroxyl groups, which are known to hydrogen bond within the emerging mesophases [9], might promote the preferential formation of aggregates and/or stabilize the mesophase [10]. Indeed, discoid supermolecules have been engineered by linking three lipophilic [*N*-monoacylated-3,3′-diamino-2,2′-bipyridine] wedges to a central 1,3,5-substituted benzenecarbonyl subunit where strong hydrogen bonds are believed to induce formation of columnar mesophases [11]. Hydrogen-bonded adducts formed between complementary 4-substituted benzoic acid proton-donating and 4,4′-bipyridine proton-accepting components are liquid crystalline at relatively high temperature [12]. It seems prudent, therefore, to equip our next-generation of metallomesogens with the necessary hydrogen-bonding functionality.

*Authors for correspondence; e-mail: ziessel@chimie.u-strasbg.fr

Journal of Liquid Crystals ISSN 0267-8292 print/ISSN 1366-5855 online © 1999 Taylor & Francis Ltd
http://www.tandf.co.uk/JNLS/lct.htm
http://www.taylorandfrancis.com/JNLS/lct.htm

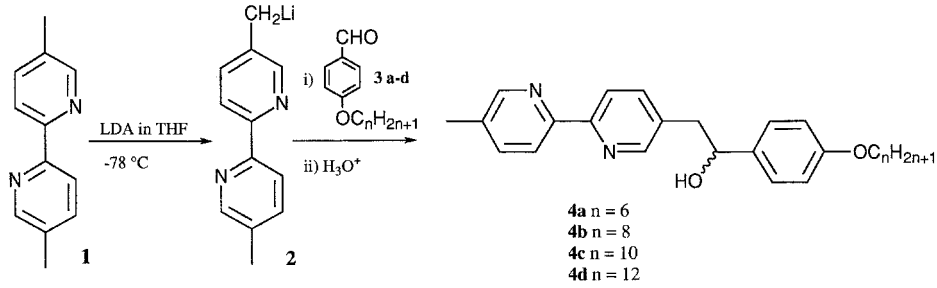

Scheme 1.

As a first step toward the preparation of such chiral metallomesogens we now report on the liquid crystallinity of a family of ligands derived from 5-methyl-5′-[2-(4-alkyloxyphenyl)-2-hydroxyethyl]-2,2′-bipyridines ($n = 6, 8, 10, 12$) and from 5-methyl-5′-[2-(4-decyloxyphenyl)ethyl]-2,2′-bipyridine. In the former series, the potential chiral centre bears an alcohol fragment and, by being sited at the molecular apex, serves to break electronic conjugation between the aromatic terminals—see structure below:

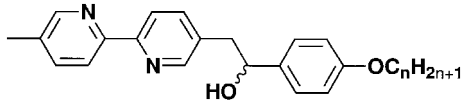

2. Synthesis and characterization

The target molecules were prepared according to scheme 1. Compounds **1** [13] and **3a–d** [14] were prepared by literature procedures. Reaction of carbanion **2** with aldehyde **3**, followed by protonation, leads to the racemic alcohol **4** in modest yield (*ca.* 60%).

The ABX signal of the bridging CH_2 group confirms the presence of an asymmetric carbon centre. Compound **6** was prepared by hydrogenation of **5** [6*a*,*b*] in the presence of Pd/C (10%) and NaH_2PO_2 as reducing agent [15], as outlined in scheme 2. All new compounds were characterized by ^{1}H NMR, $^{13}C\{^1H\}$ NMR, FTIR, and elemental analysis. Compound **6**, which bears a non-polar connecting group, was synthesized in order to study the possible role of intermolecular hydrogen bonding during formation of the mesophase.

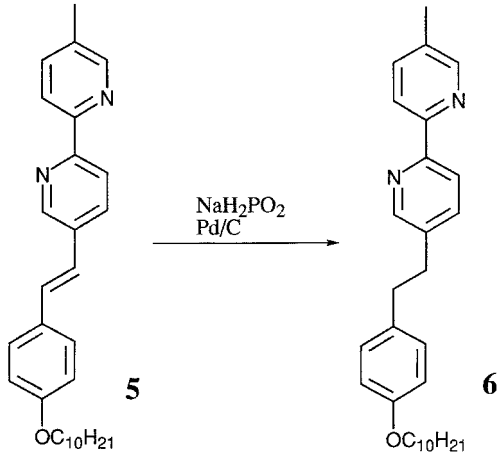

Scheme 2.

Special attention has been given to comparing transition temperatures for mesophase formation in compounds **4**, **5** and **6**. The temperature at which mesophase formation begins in **6** is significantly lower than in the other compounds studied here.

3. Results and discussion

The mesomorphic behaviour and phase transition temperatures were characterized by polarizing optical microscopy (POM), differential scanning calorimetry (DSC), and powder X-ray diffractometry (XRD). The phase transition temperatures and their corresponding enthalpy changes derived for compounds **4a–d** and **6** are compiled in table 1, while typical results are displayed in figure 1. In each case, the mesophase was confirmed by optical microscopy. The nematic phase was characterized by its schlieren texture co-existing with homeotropic alignment, while the orthogonal SmA phase was characterized by its focal-conic fan texture, also co-existing with homeotropic alignment. These mesophases were also evident in the XRD patterns, allowing determination of the *d*-spacing values for the SmA phase as listed in table 2. The SmB phase of compound **6** shows rather a high fluidity under POM and, as indicated by the XRD patterns, has an orthogonal layered structure.

According to the information shown in table 1 and displayed in figure 1, the racemic compounds **4a–d** possessing branching hydroxy groups in the linkage exhibit liquid crystalline behaviour showing SmA and N phases for the shorter chain lengths and only a SmA phase for $n = 10$ and 12. As in many homologous series, the nematic phase is favoured in those compounds (**4a** and **4b**) having relatively short terminal chains, and the somewhat longer terminal chains in **4c** and **4d** favour the SmA phase. The role, if any, of the branching hydroxy group in controlling the nature of the mesophase is not made clear from these studies and therefore

Table 1. Phase transition temperatures (°C)[a] and corresponding enthalpies (J g^{-1}) of compounds **4a–d** (n = 6, 8, 10, and 12), and **6** (n = 10).

4a	(n = 6)	Cr	97.8 (55.0) ⇌ 46.2 (31.0)		SmA	122.9 (0.7) ⇌ 120.0 (0.7)	N	143.2 (8.3) ⇌ 140.0 (9.3)		I
4b	(n = 8)	Cr	80.0 (25.0) ⇌ Supercooling		SmA	138.3 (4.4) ⇌ 134.4 (3.4)	N	147.4 (12.8) ⇌ 144.2 (10.6)		I
4c	(n = 10)	Cr	64.3 (47.9) ⇌ Supercooling		SmA	128.9 (15.3) ⇌ 119.8 (5.3)	N	⇌ 125.0 (3.2)		I
4d	(n = 12)	Cr	81.8 (61.4) ⇌ Supercooling		SmA	140.3 (10.2) ⇌ 137.1 (9.4)				I
6	(n = 10)	Cr	60.7 (25.8) ⇌ 34.2 (26.8)	SmB	72.8 (4.5) ⇌ 68.6 (4.5)	SmA	88.6 (0.5) ⇌ 84.9 (0.9)	N	106.6 (4.6) ⇌ 105.0 (6.2)	I

[a] Phase transition temperatures and corresponding enthalpies were determined from the 2nd heating and 1st cooling scans of DSC; abbreviations: Cr = crystalline phase, SmB = smectic B phase, SmA = smectic A phase, I = isotropic liquid.

Table 2. X-ray diffraction data for compounds **4a–d** and **6** in the smectic A phase.

Compound	Temperature/°C[a]	d-spacing/Å[b]	Theoretical value/Å (fully extended length)
4a (n = 6)	100	25.1 (s), 12.7 (w)	24.7
4b (n = 8)	100	27.7 (s), 14.0 (w)	27.1
4c (n = 10)	100	31.0 (s), 15.9 (w)	29.6
4d (n = 12)	100	32.6 (s), 16.5 (w)	32.0
6 (n = 10)	85	32.8 (s), 16.5 (w)	29.6

[a] All temperatures reported were measured on heating scans.
[b] s and w are strong and weak peaks, i.e. (0 0 1) and (0 0 2) reflection, respectively.

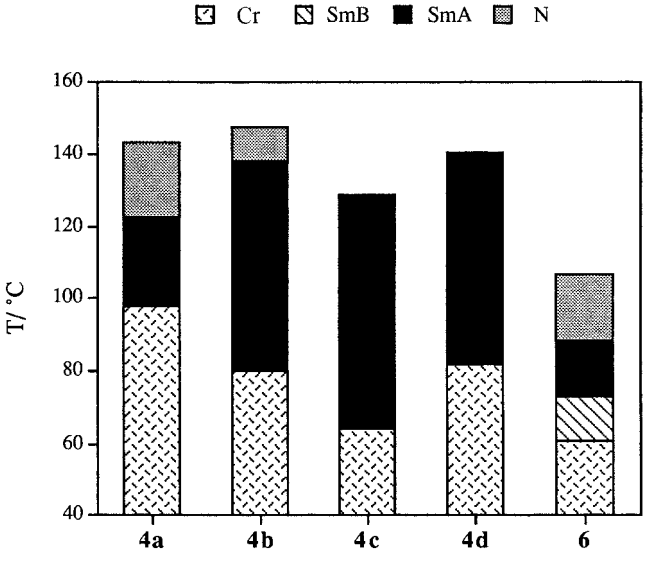

Figure 1. Phase transition temperatures (heating) of compounds **4a–d** and **6**.

a critical comparison was necessary with compound **6** where the hydroxyl function is lacking. The key comparison is between compounds **6** and **4c** and it appears that, while **6** shows distinct mesomorphic properties, **4c** possesses a significantly higher isotropization temperature. Elevation of the isotropization temperature can be attributed to intermolecular hydrogen-bonding (H-bonding) between hydroxy and pyridine groups. This effect must be sufficiently pronounced to offset the lowering of the isotropization temperature that is usually observed for liquid crystalline materials having lateral branching in either the cores or terminal chain. The layered SmA phase is also stabilized by this intermolecular H-bonding in **4c** which extends the temperature range over which this phase is dominant relative to **6**. In fact, the absence of intermolecular H-bonding in **6** and the lack of SmA stabilization favours formation of the nematic phase, but at a lower temperature than in **4a** and **4b**. This latter phase is not resolved in **4c** for the heating scan. However we note that a nematic phase is evident in the cooling scan because of greater supercooling of the N–SmA transition.

By comparison with the previously reported phase transition temperatures of the unsaturated bridge compound **5** (see [6b] and scheme 2), we can conclude that compound **6** has a shorter conjugation length, a smaller polarizability, and a somewhat less planar structure. These factors combine to ensure that compound **6** has lower isotropization temperature and narrower ranges of the SmA and nematic phases than those found for **5**.

These studies have revealed an important participation of intermolecular H-bonding in the internal organization of the mesophases for the racemic systems **4**. Further support for such interactions was sought by recording IR spectra for compounds **4a** and **4c** at temperatures corresponding to each of the various phases. The main results are displayed in figures 2 and 3, and it is clear that significant changes occur in the OH stretching band centred around 3300 cm^{-1}. This band shifts towards higher wave number as the temperature is increased, a situation entirely consistent with intermolecular hydrogen-bonding between OH and pyridino functions. The isotropic state shows the highest wave number for the OH stretch, which corresponds to relatively weak intermolecular H-bonding. For example, the OH stretch observed for compound **4a** (figure 2) occurs at 3226 cm^{-1} in the crystalline phase at 30°C, at 3271 cm^{-1} in the SmA phase at 100°C, at 3272 cm^{-1} in the nematic phase at 130°C, and at 3419 cm^{-1} in the isotropic state at 160°C. This progressive shift of the O–H stretch to higher energy with increasing temperature indicates the gradual disappearance of H-bonds as the phase becomes more disordered. Similar phenomena were observed for compound **4c** (figure 3) with the OH stretch lying at 3243, 3271 and 3392 cm^{-1}, respectively, for the crystal at 30°C, the SmA phase at 100°C, and the isotropic state at 150°C.

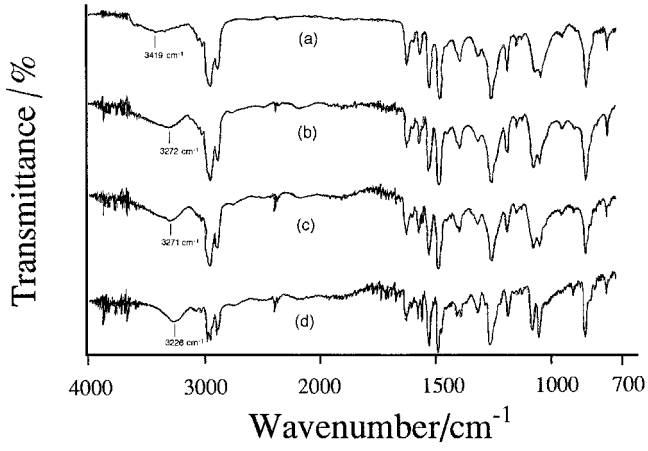

Figure 2. FTIR spectra recorded for compound **4a** (*a*) in the isotropic state at 160°C, (*b*) in the nematic phase at 130°C (*c*) in the SmA phase at 100°C, and (*d*) in the crystalline phase at 30°C.

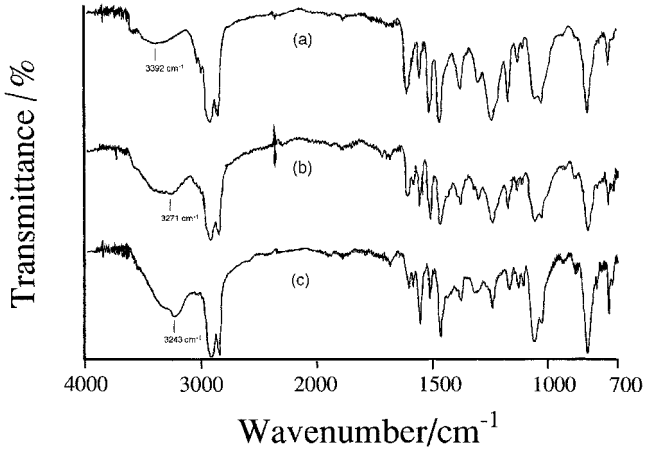

Figure 3. FTIR spectra recorded for compound **4c** (*a*) in the isotropic state at 150°C, (*b*) in the SmA phase at 100°C, and (*c*) in the crystalline phase at 30°C.

Figure 4 shows some molecular arrangements proposed tentatively on the basis of intermolecular H-bonding in racemic compounds **4a–d**. In particular, H-bonded dimers are considered in figure 4 (*a*), while a different arrangement also allowing for an orthogonal molecular orientation is considered in figure 4 (*b*). A different arrangement is shown in figure 4 (*c*) wherein a tilted molecular orientation should give rise to a SmC phase. Since only orthogonal layered SmA structures are found for compounds **4a–d**, the arrangement shown in figure 4 (*c*) seems less relevant than the other possible structures. A final head-to-tail (antiparallel) arrangement of two molecules linked by H-bonding between hydroxyl groups could not been excluded but has previously been invoked as an effective H-bonding function in liquid crystalline materials [9]. Most probably there will be a mixture of some of these idealized molecular structures within the generated mesophases.

Table 2 lists the highest XRD *d*-spacing values recorded for compounds **4a–d** and **6** in the SmA phase, together with theoretical values calculated for fully extended molecular conformations. All the XRD patterns indicate orthogonal layered structures, and there is good agreement with measured and calculated *d*-spacings. The one exception concerns compound **6** which has a larger fully extended theoretical value than the XRD *d*-spacing. In this case, the absence of hydrogen bonding might facilitate an antiparallel interdigitated packing of the molecules in the mesophase. For the racemic compounds **4a–d**, however, there is clear experimental evidence to show that intermolecular H-bonding makes a critical contribution towards the observed mesomorphic properties.

4. Conclusions

In summary, a set of asymmetric liquid crystalline compounds (**4a–d**) based on 5-methyl-5′-[2-(4-alkyloxyphenyl)-2-hydroxyethyl]-2,2′-bipyridines has been synthesized while the related compounds **5** and **6** allow detailed examination of how an asymmetrical central linkage containing a branching hydroxy group affects the mesomorphic properties of the racemic materials. It is seen clearly that the presence of an sp^3 carbon atom in the central linkage of **6** induces a significant decrease

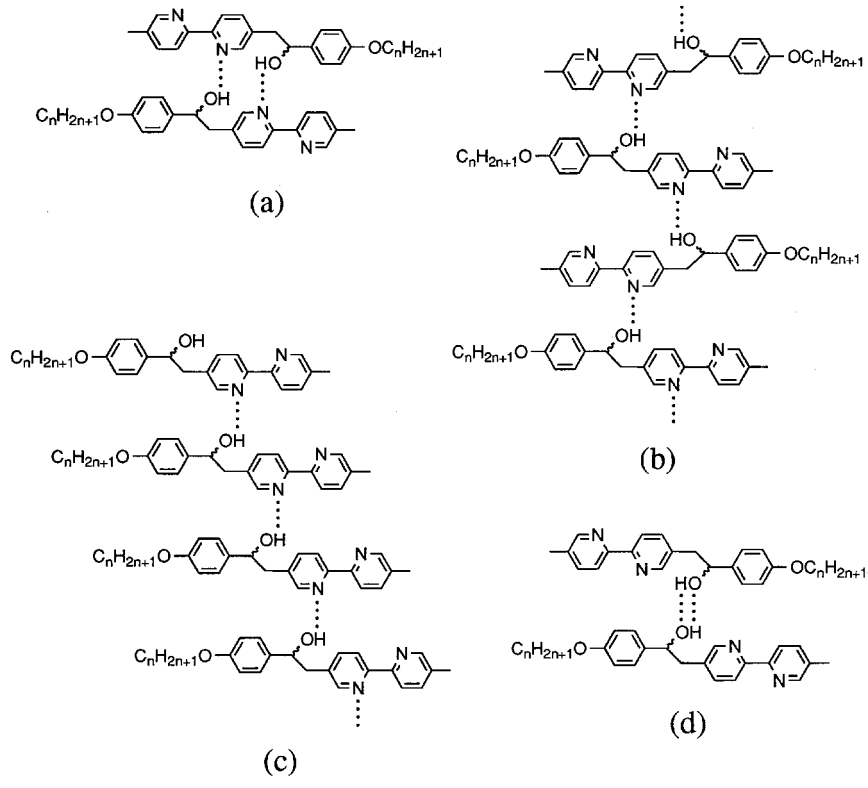

Figure 4. Postulated molecular packing induced by intermolecular H-bonding (·····) for compounds **4a–d** ($n = 6$–12) in the mesophases generated.

in the temperatures at which isotropization and mesophase formation take place. Further comparison of the results derived for compounds **4a–d** and **6** indicates the importance of a central branching hydroxy function. It appears that this latter group favours intermolecular hydrogen bonding in **4a–d** in such a way as to stabilize the orthogonal layered SmA phases, whilst destabilizing the nematic phase by restricting lateral hydrogen bonding. Continuing studies are attempting to employ related chiral bidentate molecules and their transition metal complexes as a means by which to extend the known range of liquid crystalline materials.

5. Experimental

5.1. *General*

All reactions were performed under argon in Schlenk flasks. THF was dried over sodium/benzophenone and distilled under argon before use. Infrared spectra were recorded in the region 4000–400 cm^{-1} with a Bruker IFS-66 FTIR spectrometer. ^1H (200 MHz) and $^{13}C\{^1H\}$ (50.3 MHz) NMR spectra were recorded at room temperature with a Bruker AC-200 instrument. Deuteriated chloroform was used as a solvent and internal standard: δ(H) in ppm are relative to residual protiated solvent (7.26) and δ(C) in ppm are relative to $CDCl_3$ (77.03). Thermal transition temperatures were derived from studies made with a Perkin-Elmer DSC 7, whilst the corresponding textures were imaged with a Leitz Laborlux S polarizing optical microscope (POM) equipped with a THMS-600 heating stage. Heating and cooling rates were 10°C min^{-1}, unless stated otherwise. Powder X-ray diffraction (XRD) patterns were obtained with a Siemens D-5000 (40 kV, 30 mA) X-ray diffractometer fitted with a TTK450 temperature controller. Nickel-filtered CuK_α radiation was used as the incident X-ray beam. The temperature depndence of the IR spectra was studied with a Perkin-Elmer IR microscope (Auto-image) equipped with an FTIR 600 heating stage attached directly to a Perkin-Elmer Spectrum 2000 FTIR spectrometer. A total of 64 individual spectra were accumulated at a resolution of 4 cm^{-1} in the range 4000–700 cm^{-1} with a spot diameter of $100 \times 100\ \mu m^2$.

5.2. *Synthesis*

5.2.1. *5-Methyl-5′-[2-(4-hexyloxypheny l)-2-hydroxyethyl]-2,2′-bipyridine* ***4a*** *(and higher homologues)*

A solution of *n*-butyl lithium in hexane (5.8 ml, 1.57M, 8.14 mmol) was added slowly to a solution of di-isopropylamine (1.2 ml, 8.14 mmol) in THF (25 ml) maintained at − 78°C. After 0.5 h, solid 5,5′-dimethyl-2,2′-bipyridine (1.5 g, 8.14 mmol) was added carefully to the stirred solution, which immediately turned a deep

brown–purple colour. After stirring for a further 1 h at − 78°C, a solution of 4-hexyloxybenzaldehyde (1.05 eq, 8.55 mmol) in THF (5 ml) was added to the solution via a cannula tube. Stirring was continued for 0.25 h before the solution was allowed to reach room temperature. The resultant orange-coloured solution was stirred overnight and subsequently neutralized with an aqueous solution of NH_4Cl, during which the solution turned yellow and NH_3 gas was evolved. The solvent was evaporated under vacuum and the yellow residue dissolved in CH_2Cl_2 before being purified by column chromatography on silica, eluting first with CH_2Cl_2 to remove unreacted 5,5′-dimethyl-2,2′-bipyridine and then with CH_2Cl_2/MeOH, 95/5, v/v to isolate the required product. The white product was collected ($R_f = 0.43$, silica, CH_2Cl_2/MeOH, 95/5), yield 2.192 g, 69%. Elemental analysis: calc. for $C_{25}H_{30}N_2O_2$ ($M_r = 390.530$) C 76.89, H 7.74, N 7.17; found C 76.68, H 7.59, N 6.90%. IR (KBr): 3226 (s broad), 2924 (s), 2859 (s), 1610 (m), 1510 (s), 1469 (s), 1238 (s), 1069 (s). ^{1}H NMR ($CDCl_3$) δ 0.91 (t, 3H, CH_3 alkyl, $^3J(HH) = 6.6$ Hz), 1.35 (s broad, 6H, $(CH_2)_3$ alkyl), 1.73 (m, 2H, OCH_2CH_2 alkyl), 2.28 (s, 3H, CH_3 bipy), 2.98 (m, 2H, CH_2 bipy), 3.88 (t, 2H, CH_2 alkyl, $^3J(HH) = 6.3$ Hz), 4.1 (s broad, 1H, OH, exchange with D_2O), 4.73 (t, 1H, $CHOH$, $^3J(HH) = 6.3$ Hz), 6.97 (AB system, 4H, $CH_{aromatic}$, $J(AB) = 7.8$ Hz, $\Delta\nu = 73.5$ Hz), 7.48 (dd, 2H, $H_{4\text{ and }4'\text{ bipy}}$, $^3J(HH) = 8.2$ Hz, $^4J(HH) = 2.4$ Hz), 8.12 (d, 2H, $H_{3\text{ and }3'\text{ bipy}}$, $^3J(HH) = 8.1$ Hz), 8.29 (s, 2H, $H_{6\text{ and }6'\text{ bipy}}$). $^{13}C\{^1H\}$ NMR ($CDCl_3$) δ 13.88 (CH_3 alkyl), 18.08 (CH_3 bipy), 22.45, 25.58, 29.11, 31.45, (CH_2 alkyl), 42.48 (CH_2 bipy), 67.86 (OCH_2), 74.07 (CHOH), 114.17, 120.15, 120.41, 127.0, 132.90, 133.89, 135.78, 137.27, 137.9, 149.26, 149.85, 153.35, 153.94, 158.46, ($C_{aromatic}$).

5.2.2. *5-Methyl-5′-[2-(4-octyloxyphenyl)-2-hydroxyethyl]-2,2′-bipyridine* ***4b***

$R_f = 0.43$, silica, CH_2Cl_2/MeOH, 95/5, yield 2.11 g, 62%. Elemental analysis: calc. for $C_{27}H_{34}N_2O_2$ ($M_r = 418.169$) C 77.48, H 8.19, N 6.69; found C 77.60, H 8.09, N 7.01%.

5.2.3. *5-Methyl-5′-[2-(4-decyloxyphenyl)-2-hydroxyethyl]-2,2′-bipyridine* ***4c***

$R_f = 0.43$, silica, CH_2Cl_2/MeOH, 95/5, yield 1.998 g, 55%. Elemental analysis: calc. for $C_{29}H_{38}N_2O_2$ ($M_r = 446.638$) C 77.99, H 8.58, N 6.28; found C 77.83, H 8.41, N 6.19%.

5.2.4. *5-Methyl-5′-[2-(4-dodecyloxyphenyl)-2-hydroxyethyl]-2,2′-bipyridine* ***4d***

$R_f = 0.43$, silica, CH_2Cl_2/MeOH, 95/5, yield 2.20 g, 57%. Elemental analysis: calc. for $C_{31}H_{42}N_2O_2$ ($M_r = 474.692$) C 78.44, H 8.92, N 5.90; found C 78.39, H 8.74, N 6.33%.

5.2.5. *5-Methyl-5′-[2-(4-dodecyloxyphenyl)ethyl]-2,2′-bipyridine* ***6***

A solution of sodium phosphinate (H_2PO_2Na) (700 mg, 7.97 mmol) in H_2O (10 ml) was added to a solution of compound **5** (60 mg, 14 mmol) in THF (30 ml) before addition of a suspension of Pd/C (10%) catalyst (60 mg). The mixture was heated at reflux for 3 days with constant agitation. After cooling to rt, the solution was filtered before evaporation of the THF *in vacuo*. The remaining aqueous phase was shaken with CH_2Cl_2 (3 × 20 ml) and the organic extract dried over $MgSO_4$ and evaporated to dryness. The solid was purified by column chromatography on silica (CH_2Cl_2/hexane, 70/30, v/v as eluant). The white product was collected ($R_f = 0.39$, silica, CH_2Cl_2/hexane, 70/30), yield 50 mg, 83%. Elemental analysis: calc. for $C_{29}H_{38}N_2O$ ($M_r = 430.639$) C 80.89, H 8.89, N 6.51; found C 80.68, H 8.76, N 6.42%. IR (KBr): 2919 (s broad), 2850 (s), 1508 (s), 1486 (s), 1235 (s), 1027 (s), 828 (s). ^{1}H NMR ($CDCl_3$) δ 0.88 (t, 3H, CH_3 alkyl, $^3J(HH) = 6.3$ Hz), 1.27 (s broad, 14H, $(CH_2)_7$ alkyl), 1.74 (m, 2H, OCH_2CH_2 alkyl), 2.37 (s, 3H, CH_3 bipy), 2.85 and 2.90 (s, 4H, CH_2CH_2 link), 3.0 (t, 2H, OCH_2 alkyl, $^3J(HH) = 6.5$ Hz), 6.92 (AB system, 4H, $H_{aromatic}$, $J(AB) = 8.5$ Hz, $\Delta\nu = 98.1$ Hz), 7.56 (dd, 2H, $H_{4\text{ and }4'\text{ bipy}}$, $^3J(HH) = 8.2$ Hz, $^4J(HH) = 1.6$ Hz), 8.24 (d, 2H, $H_{3\text{ and }3'\text{ bipy}}$, $^3J(HH) = 8.2$ Hz), 8.46 (dd, 2H, $H_{6\text{ and }6'\text{ bipy}}$, $^4J(HH) = 1.6$ Hz). $^{13}C\{^1H\}$ NMR ($CDCl_3$) δ 14.06 (CH_3 alkyl), 18.26 (CH_3 bipy), 22.63, 26.02, 29.29, 29.35, 29.54, 31.86 (CH_2 alkyl), 34.95 (CH_2 link), 36.49 (CH_2 link), 67.95 (OCH_2), 114.43, 120.29, 129.32, 127.14, 132.60, 132.97, 136.76, 136.86, 137.33, 149.25, 149.50, 153.70, 154.14, 157.55, 173.43 ($C_{aromatic}$).

This work was supported, in part, by the Centre Nationale de la Recherche Scientifique (CNRS) and by the Ecole de Chimie, Matériaux, et Polymères (ECPM). We thank Dr Antoine Skoulios for many helpful discussions.

References

[1] Goodby, J. W., Slaney, A. J., Booth, C. J., Nishiyama, I., Vuijk, J. D., Styring, P., and Toyne, K. J., 1994, *Mol. Cryst. liq. Cryst.*, **243,** 231 and references cited therein.

[2] (*a*) Giroud-Godquin, A. M., and Maitlis, P. M., 1991, *Angew. Chem. int. Ed. Engl.*, **30,** 375; (*b*) Espinet, P., Esteruela, M. A., Oro, L. A., Serrano, J. L., and Sola, E., 1992, *Coord. Chem. Rev.*, **117,** 215; (*c*) Bruce, D. W., 1993, *Inorganic Materials*, edited by D. W. Bruce and D. O'Hare (Chichester: Wiley).

[3] Serrano, L., and Sierra, T., 1996 in *Metallomesogens*, edited by L. Serrano (Weinheim: VCH), pp. 107–111.

[4] Kuboki, T., Araki, K., Yamada, M., and Shiraishi, S., 1994, *Bull. chem. Soc. Jpn.*, **67,** 948.

[5] (*a*) Bruce, D. W., and Rowe, K. E., 1995, *Liq. Cryst.*, **18,** 161; (*b*) Bruce, D. W., and Rowe, K. E., 1996, *Liq.*

Cryst., **20,** 183; (*c*) BRUCE, D. W., and ROWE, K. E., 1995, *J. chem. Soc. Dalton Trans*., 3913.

[6] (*a*) DOUCE, L., ZIESSEL, R., SEGHROUCHNI, R., SKOULIOS, A., CAMPILLOS, E., and DESCHENAUX, R., 1995, *Liq. Cryst*., **18,** 157; (*b*) DOUCE, L., ZIESSEL, R., SEGHROUCHNI, R., SKOULIOS, A., CAMPILLOS, E., and DESCHENAUX, R., 1996, *Liq. Cryst*., **20,** 235; (*c*) EL-GHAYOURY, A., DOUCE, L., ZIESSEL, R., SEGHROUCHNI, R., and SKOULIOS, A., 1996, *Liq. Cryst*., **21,** 143.

[7] EL-GHAYOURY, A., DOUCE, L., ZIESSEL, R., and SKOULIOS, A., 1998, *Angew. Chem. int. Ed. Engl*., **37,** 1255.

[8] EL-GHAYOURY, A., DOUCE, L., ZIESSEL, R., and SKOULIOS, A., 1998, *Angew. Chem. int. Ed. Engl*., **37,** 2205.

[9] PLEHNERT, R., SCHRÖTER, A., and TSCHIERSKE, C., 1998, *J. mater. Chem*., **8,** 2611.

[10] SUAREZ, M., LEHN, J.-M., ZIMMERMAN, C., SKOULIOS, A., and HEINRICH, B., 1998, *J. Am. chem. Soc*., **120,** 9526.

[11] PALMANS, A. R. A., VEKEMANS, J. A. J. M., FISCHER, H., HIKMET, R. A., and MEIJER, E. W., 1997, *Chem. Eur. J*., **3,** 300.

[12] PRICE, D. J., ADAMS, H., and BRUCE, D. W., 1996, *Mol. Cryst. liq. Cryst*., **289,** 127.

[13] BADGER, G. M., and SASSE, W. H. F., 1956, *J. chem. Soc. chem. Commun*., 616.

[14] WEYGAND, C., and GABLER, R., *J. prakt. Chem*., **155,** 332.

[15] JOHNSTONE, R. A. W., and WILBY, A. H., 1981, *Tetrahedron*, **37,** 3667.